Avaliação de nanofluidos de nanoargila montmorilonita hidrofílica e goma xantana em meio salino

Evaluation of hydrophylic montmorillonite nanofluids and xantane gum in saline environment

Evaluación de nanofluidos de montmorillonita hidrofílica y goma de xantano en salina

Felipe Menezes de Souza
ORCID: https://orcid.org/0000-0002-6686-6320
Universidade Federal da Bahia, Brazil
E-mail: felipemenezessouza@gmail.com

Juliana Mikaelly Dias Soares
ORCID: https://orcid.org/0000-0003-2832-3461
Universidade Federal do Vale do São Francisco, Brazil
E-mail: juliana_mikaelly@hotmail.com.br

Helinando Pequeno de Oliveira
ORCID: https://orcid.org/0000-0002-7565-5576
Universidade Federal do Vale do São Francisco, Brazil
E-mail: helinando@gmail.com

Isabel Cristina Rigoli
ORCID: https://orcid.org/0000-0002-7042-2087
Universidade Federal da Bahia, Brazil
E-mail: irigoli@ufba.br

Samuel Luporini
ORCID: https://orcid.org/0000-0003-4334-5343
Universidade Federal da Bahia, Brazil
E-mail: sam5luporini@uol.com.br

Resumo

Com a estimativa de aumento da demanda de petróleo para as próximas décadas, intensifica-se a necessidade de exploração de áreas não convencionais, e associada a elas, ante aos altos custos de exploração, a necessidade de aperfeiçoar as tecnologias

disponíveis. Nesse sentido, na última década, intensificou-se a aplicação de nanopartículas para o aperfeiçoamento de fluidos de perfuração. Nesse cenário, as nanoargilas montmorilonitas e as gomas xantana foram pouco exploradas para o desenvolvimento de nanofluidos. Neste trabalho, verificou-se a influência da nanoargila montmorilonita hidrofílica sobre os parâmetros reológicos de soluções de xantana, cloretos de sódio e de cálcio. Para tal, primeiro, a argila foi caracterizada por DRX, FRX e TGA. Depois, mantendo constantes as concentrações dos sais e da xantana, avaliou-se a influência da variação de concentração de nanoargila sobre a reologia da solução. Em seguida, mantendo as concentrações dos componentes constantes, verificou-se a influência da temperatura e em seguida do tempo de hidratação sobre a reologia da mistura. Por fim, para avaliar a interação das partículas da mistura, verificou-se a Condutividade Elétrica e o Potencial Zeta, variando-se concentração de nanoargila e tempo de hidratação. Concluiu-se que: para certas concentrações de nanoargila, há melhoria da reologia das soluções de xantana; a adição de nanoargila favorece a reologia na mistura de xantana com o aumento da temperatura; o tempo de hidratação não afeta significativamente a reologia do nanofluido; há interação entre a nanoargila e a xantana.

Palavras-chave: Nanoargila; Xantana; Nanofluido de perfuração; Reologia.

Abstract

With an estimated increasing oil demand in the coming decades, the need to explore non-applicable areas is intensified, and associated with them, before the high exploration costs, the need to improve available technologies. In this sense, in the last decade, the application of nanoparticles to improve drilling fluids has been intensified. In this scenario, montmorillonite nanoclays and xanthan gums were little explored for the development of nanofluids. In this work, the influence of hydrophilic nanoclay on the rheological parameters of xanthan, sodium and calcium chlorides solutions was verified. For this, first, the clay was characterized by XRD, XRF and TGA. Then, maintaining constant the salt and xanthan concentrations, the influence of the variation in the concentration of nanoclay on the rheology of the solution was evaluated. Then, keeping the components concentrations constant, the influence of temperature was verified and then the hydration time on the rheology of the mixture. Finally, to assess the interaction of the mixture, it was verified the Electrical Conductivity and the Potential Zeta, varying the concentration of the nanoclay and the hydration time. It was concluded that: for certain nanoclay concentrations, there is an improvement in the rheology of xanthan solutions;

an addition of nanoclay favors rheology in the mixture of xanthan with increased temperature; hydration time does not affect the rheology of the nanofluid; there is interaction between nanoclay and xanthan.

Keywords: Nanoclay; Xanthan; Drilling nanofluid; Rheology.

Resumen

Con el aumento estimado de la demanda de petróleo para las próximas décadas, la necesidad de exploración de áreas no convencionales se intensifica, y asociada con ellas, dados los altos costos de exploración, la necesidad de mejorar las tecnologías disponibles. En este sentido, en la última década, la aplicación de nanopartículas para la mejora de los fluidos de perforación se ha intensificado. En este escenario, las nanoarcillas de montmorillonita y las gomas de xantano se exploraron poco para el desarrollo de nanofluidos. En este trabajo, se verificó la influencia de la nanoarcilla hidrofílica de montmorillonita en los parámetros reológicos de las soluciones de cloruros de xantano, sodio y calcio. Para esto, primero, la arcilla se caracterizó por DRX, FRX y TGA. Luego, manteniendo constantes las concentraciones de sales y xantano, se evaluó la influencia de la variación en la concentración de nanoarcilla en la reología de la solución. Luego, manteniendo constantes las concentraciones de los componentes, se verificó la influencia de la temperatura y luego el tiempo de hidratación en la reología de la mezcla. Finalmente, para evaluar la interacción de las partículas en la mezcla, se verificó la conductividad eléctrica y el potencial Zeta, variando la concentración de nano arcilla y el tiempo de hidratación. Se concluyó que: para ciertas concentraciones de nanoarcilla, hay una mejora en la reología de las soluciones de xantano; la adición de nanoarcilla favorece la reología en la mezcla de xantano con el aumento de la temperatura; el tiempo de hidratación no afecta significativamente la reología del nanofluido; Existe una interacción entre nano-arcilla y xantano.

Palabras clave: Nanoarcilla; Xantano; Nanofluido de perforación; Reología.

1. Introduction

Global oil demand is estimated to grow at 2% per year until 2030, with Asian countries consumption growing by 3.7% per year (EIA, 2006). It is also estimated that, in 2040, half of the world population will have its energy demand supplied by oil, with an increase of 28% in relation to the current demand (EIA, 2017). This scenario directs

the oil industry to unconventional exploration zones, which offer greater challenges to its production, such as deeper environments, greater fragility of the reservoir rock, high temperature and pressure (HT/HP) (Aftab, et al, 2017; Al-Yasiri & Al-Sallami, 2015). These peculiarities are reflected in the operating cost, which ranges from £ 20 to 25 million per well, but can reach £ 40 million per well (Fitzgerald et. al., 2000). However, drilling fluids, which are primarily responsible for lubricating and cooling drill components, sealing the well wall and raising cuttings to the surface (Caenn et al., 2014), correspond to 25% of operating costs (Khodja et al., 2010) and, given the complexity of the wells in unconventional zones, these fluids need to be improved (Amanullah et al., 2011; Al-Yasiri et al., 2019).

Therefore, the use of nanoparticles in the improvement of drilling fluids has been the subject of research in the last decade (Perween et al., 2019; Al-Yasiri & Al-Sallami, 2015; Al-Yasiri et al., 2019). Nanoparticles are materials whose size ranges from 1 to 100nm (Dolez, 2015). Given the surface area/particle volume ratio, nanoparticles can significantly contribute to changing the properties of drilling fluids with little addition of material (Al-Yasiri & Al-Sallami, 2015). For example, Abdou and Ahmed (2011), Li et al. (2016), Srivatsa & Ziaja (2011), Contreras et al. (2014) and Barry et al. (2015) adopted nanoparticles to reduce and control the filtrate. Willian et al. (2014) applied CuO and ZnO nanoparticles to improve the thermal and electrical conductivity of drilling fluids. Jain and Mahto (2015), Hoelscher et al. (2012) and Riley et al. (2012) applied nanoparticles to improve shale stability. Cheraguian et al. (2018) and Alizadeh et al. (2015) applied nanoparticles to improve the rheological behavior of drilling fluids.

Among the different types of nanoparticles, nanoclays have been widely used for the enhancement of materials (Uddin, 2008; Amiri & Sadeghialiabadi, 2014; Mélo et al., 2014). Among them, due to their low cost and abundance (Amiri & Sadeghialiabadi, 2014; Mélo et al., 2014; Nejad et al. 2011), their physical-chemical characteristics (Golubeva et al. 2013) and modification capacity for interaction with polymers (Vipulanandan & Mohammed, 2015; Mélo et al., 2014), montmorillonite (NA) nanoclays are the most required. Their use extends to the development of microporous nanocomposites used in separation filters, catalysts, cell scaffolds (Liu et al., 2011), development of nanofilms for the food industry (Tang et al., 2008; Nejad et al. 2011; Slavutsky et al., 2012), of biodegradable materials (Yang et al., 2007; Chung and Lai, 2010), wastewater treatment (Wang et al., 2017), modifications of construction materials (You et al., 2011), improvement of polymer blends (Santos et al. 2016; Mélo et al., 2014;

Gierszewska et a., 2019), application in drugs (Villaça et al., 2014; Khunawattanakul et al., 2010; Noori eta at., 2015), among others. In drilling fluids, NA was applied to improve rheological and filtrate properties in fluids based on bentonite and polymeric additives (Shakib et al., 2016; Cheraghian (2017)); Jain and Mahto (2015) added NA to polyacrylamide to inhibit shale; Hassani and Ghazanfari (2017) applied NA for the development of colloidal gas aphrons for application in drilling fluids; Vipulanandan and Mohammed (2015) applied NA in bentonite based sludge to improve rheology and electrical resistivity. However, the application of NA to the perfection of drilling fluids is still discreet when compared to other nanoparticles or in other segments.

At the same time, the use of nanoparticles associated with polymer-based fluids is small compared to those of bentonite (Vryzas & Kelessidis, 2017; Aftab et al., 2017). Usually associated with clay sludge, polymers accumulate multiple functions in drilling fluids, such as viscosifiers, filtrate tuners, well wall stabilizers, shale swelling inhibitors, etc., but their properties are sensitive to high temperatures (Caenn et al, 2014; Lucena et al., 2014). As an example of polymer-based nanofluids, Ismail et al. (2016) applied carbon nanotubes and nano-silicon associated with polyonic cellulose and polyacrylamide; Parizad et al. (2018) applied titanium nano-oxide in mud based on xanthan, polyacrylamide and carboxymethylcellulose; Sadeghalvaad and Sabbaghi (2015) applied titanium nano-oxide to polyacrylamide sludge; Fakoya and Shah (2013) used silica nano-oxide and a mixture of surfactant and guar gum.

In this context, xanthan gum (XG), applied since the 1960s in the oil sludge industry (Caenn et al. 2014; Reinoso et. al., 2014), has viscosifying properties, pseudoplastic behavior at low concentrations, reduced filtrate loss, resistance to bacterial degradation, resistance to a wide pH range and salt concentration (Caenn et al., 2014; Howard et al., 2015; Jang et al., 2015; Kelco, 2000). Associated with nanoparticles, XG has been applied to drug development (Kennedy et al., 2015; Pooja et al., 2014), in the food industry (Taheri and Jafari, 2019), biodegradable materials (Melo et al., 2011), porous barriers for environmental decontamination (Comba et. al., 2011), among other uses. However, in the development of nanofluids (Amanullah et al., 2011), they are still associated with bentonite sludge or are rarely applied as a major component of the sludge. For example, Ponmani et al. (2014) applied CuO and nanoparticulate ZnO to improve electrical and thermal conduction of XG fluids; Perween et al. (2019) used nanoparticulate $BiFeO_3$ to improve rheological properties and XG-based sludge filtrate; Srivatsa and Ziaja (2011) applied SiO_2 nanoparticles and surfactants to improve filtrate

control; Soliman et al. (2020) promoted XG modification by reaction with nanoparticulate SiO_2 to improve rheological properties, resistance to thermal degradation and wettability in rock. However, given its properties, its use has great potential for application.

Hence, the interaction of NA and XG in saline solutions was studied, evaluating the rheological behavior, stress relationship and shear rate. For this, first, the nanoparticle was characterized. Then, by varying the NA concentration at a temperature of 25°C, the rheological interaction profile, the rheological parameters of these profiles and the influence of the NA concentration on the respective ones were determined. Then, selecting an NA concentration, the influence of temperature on the rheological profile and its parameters was evaluated. Then, maintaining the concentration of the components of the mixture, the hydration time of the samples and the effect on the reference parameters were varied. Finally, the interaction of the particles of NA and XG in saline environment was evaluated, verifying the influence of concentration and hydration time on the stability of these interactions.

2. Methodology

Similar to previous authors (Amanullah et al., 2011; Ponmani et al., 2014; Perween et al., 2019; Soliman et al., 2020; Ismail et al., 2016; Parizad et al., 2018), in this experimental research, the interaction between NA, XG and sodium and calcium salts were evaluated quantitatively (Prodanov and Freitas, 2013). This test was divided into stages: in the first, NA was characterized by X-Ray Diffraction (XRD), X-Ray Fluorescence (XRF) and Thermogravimetry (TG); in the second, the rheological parameters of the mixture were evaluated, varying the concentration of NA and keeping the concentrations of XG, Sodium Chloride (NaCl), Calcium Chloride ($CaCl_2$) and temperature at 25ºC constant; in the third, keeping the concentration of substances constant and adopting a reference NA concentration, the rheological parameters were again evaluated by varying the temperature; in the fourth, keeping the concentration of the mixture components and the temperature at 25ºC constant, the influence of the hydration time on the rheological parameters was evaluated for a time interval of 24h and 144h. In the fifth, three samples with different rheological parameters were first selected and Electrical Conductivity and Zeta Potential were evaluated; then, maintaining the concentration of the sample from step four, Conductivity and the Zeta Potential were varied and measured for samples with hydration time varying between 24 and 144h.

For the tests, Sigma Aldrich Hydrophilic Montmorillonite Nanoclay, Synth Xanthan Gum 200 MESH, Synth Sodium Chloride (NaCl) and Sigma Aldrich Calcium Chloride P.A. (CaCl$_2$) were used. To characterize the NA sample, a Shimadzu X-Ray Diffractometer, model XRD 7000, a Bruker X-Ray Fluorescence instrument, model FRX S2 Ranger, and a Shimadzu thermogravimetric analyzer, model TGA-51-H were used. For sample preparation, a BEL Engineering Analytical Scale, model S423, a Fisatom Mechanical Stirrer, model 715 were also used. For the viscosity tests, the Haake viscometer was used. For the Zeta Potential and Electrical Conductivity tests, Malvern's Zetasizer nano ZS90 analyzer was used.

For sample preparation, the components were added in the following sequence: distilled water was added to the beaker in 50% of the total sample volume; XG was added and stirred for 10 minutes; then, NA was added and stirred for another 10 minutes; then, NaCl was added and the mixture was stirred for 5 minutes; finally, CaCl$_2$ was added and the mixture was stirred for another 5 minutes. The sample volume was completed with distilled water and then the sample was stirred for 1 minute. In all stages, the mixtures were stirred between 1000 and 1500 rpm. The samples were kept at 4 ° C for 24 hours and then analyzed.

The rheological model adopted for the tests was that of Herschel-Bulkley (Herschel and Bulkley, 1926), adopted for fluids that add Bingham's pseudoplastic and plastic properties, extensively applied in clay-based fluid modeling (Kelessidis et al., 2006; Kelessidis et al., 2007, Kelessidis and Maglione, 2008), but already adopted in studies of XG rheology in concentrations that show shear thinning (Holme et al., 1988; Khalil and Jan, 2012). The model follows the following equation:

$$\tau = \tau_0 + k(\dot{\gamma})^n \qquad \qquad \text{(Eq.1)}$$

where τ_0 represents the Minimum Stress to the flow of the fluid, n is the Behavior Index of the mixture and k is the Consistency Index. The first parameter represents the resistance of the fluid to start the flow, the second parameter is associated with the thinning of the fluid with the increase of the shear rate, and the third parameter the apparent viscosity of the fluid (Herschel and Bulkley, 1926; Kelessidis et al., 2006; Kelessidis et al., 2007; Kelessidis and Maglione, 2008; Khalil and Jan, 2012). All tests were done in triplicate. To determine the rheological parameters, non-linear regression of

the results obtained on the viscometers was performed using the *Origin Pro 2017®* software.

3. Results and discussions

3.1. Part 1

The XRD test was performed with a copper anode at 40kV and a current of 45mA, with a step of 1.2°/min under continuous scanning. The results are shown in Figure 1. The test shows peaks at 5.95°, 26.99º, 41.99º, and the peaks between 70 and 80° belonging to Calcium Montmorillonite; the peaks of the order of 17º, 19.70º, 34.94º, 54.14 ° and 61.75° are from Sodium Montmorillonite; the other peaks of Beidellite. This composition shows that it is a so-called "natural" clay and considering that Beidellite is a sodium aluminosilicate, the analyzed clay has a higher sodium content than calcium, making it the sodium type (Santos, 1989; Grim and Güven, 1978). It is observed that the peak at 5.95°, corresponding to the basal layer with baseline reflection d001 (Santos, 1989), has an interlayer spacing of 14.85Å, meaning the existence of double layers of water (Sato et al., 1992; Laird, 2006), under a relative humidity of 40% for montmorillonites with calcium as free cation (Laird, 2006; Oueslati et al., 2015), confirming the identification of the mineral clay. Despite the possibility that the peaks detected between 20° and 30° are associated with the presence of quartz, mica and kaolinite (Souza, 1989; Morita et al., 2015; Menezes et al., 2008), the peak of the order of 29.04° and 40.24° is characteristic of Beidellite (Grim and Güven, 1978).

Figure 1 – NA X-Ray Diffractogram.
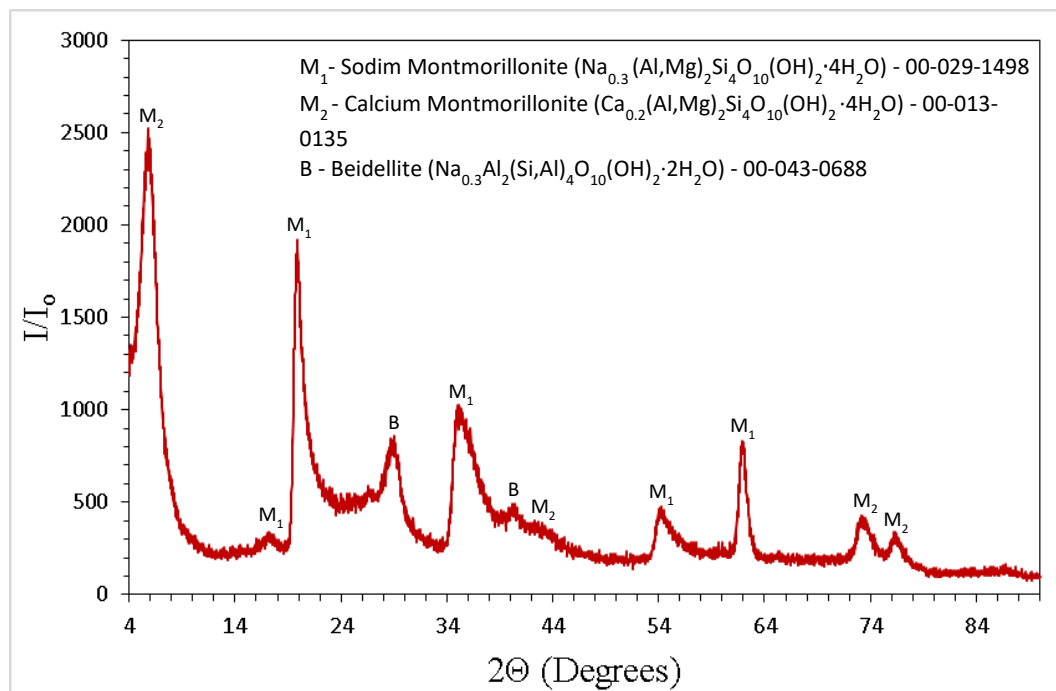
Source: Authors.

The chemical composition of the sample, obtained by FRX, is shown in Table 1. The high concentration of SiO_2 indicates the presence of free silica (Gaidzinski et al., 2009), and the concentration of Al_2O_3 is in agreement with montmorillonites (Santos, 2000). The low concentration of CaO associated with a high concentration of MgO points to the presence of carbonates (Monteiro and Vieira, 2004), and the high concentration of MgO confirms the classification of mineral clay (Santos, 2000). The ratio between Na_2O and CaO concentrations is 1.88, indicating that sodium montmorillonite type (Santos, 2000). The low concentration of K_2O preserves the rheological behavior of the clay by preventing the formation of crystalline structure under slight heating of the clay (Amorim, 2003). The low concentration of TiO_4 shows that such an oxide does not interfere with the properties of the clay (Santos, 2000).

The thermigravimetric analysis is shown in Figure 2. Two endothermic peaks are observed at less than 100°C, corresponding to free adsorbed water (Santos, 1989; Xie et al., 2001; Mariani et al., 2013). There is an endothermic peak in the order of 260°C, which corresponds to dehydroxylation of amorphous aluminum hydroxides. The endothermic peak in the order of 700°C corresponds to the loss of structural hydroxyls (Santos, 1989).

Table 1- NA X-Ray Fluorescence Test.

Components	Amount (m/m)
Na_2O	3.20%
MgO	7.10%
Al_2O_3	20.70%
SiO_2	62.32%
SO_3	0.26%
Cl	0.34%
K_2O	0.20%
CaO	1.70%
TiO_2	0.39%
Fe_2O_3	3.52%
ZrO_2	0.10%

Source: Authors.

Figure 2 – Thermogravimetric Test.
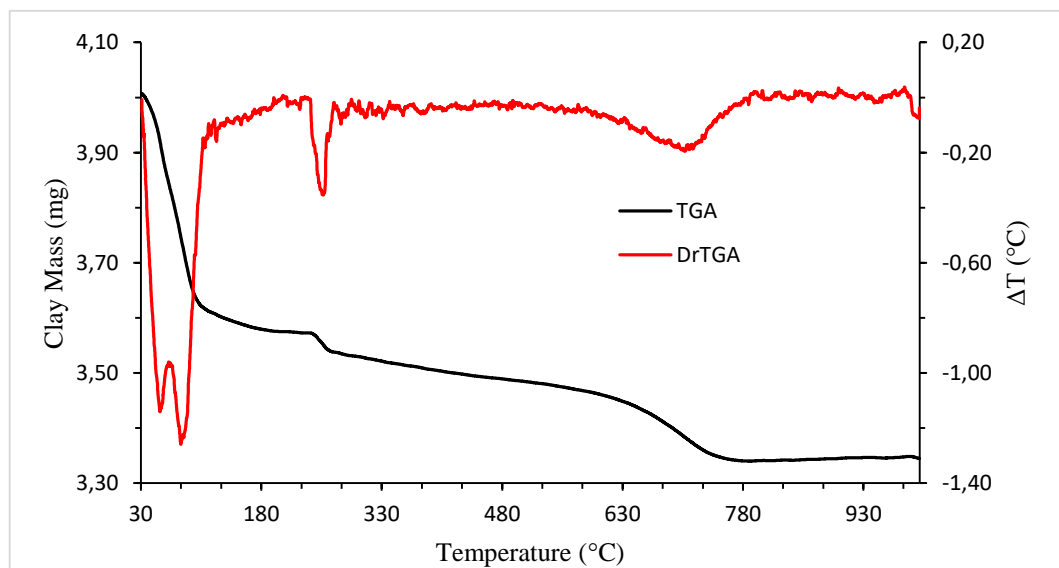
Source: Authors.

3.2. Part 2

For the second part, the concentrations of XG, NaCl and $CaCl_2$ were maintained at 0.51% w/v, 12.86% w/v and 0.414% w/v, respectively. At this concentration, above the limit concentration, XG in water is salt-free and has a tangle conformation (Wyatt et

al., 2011), characterized by the prevalence of hydrogen bonds between the disordered anionic chains of biopolymer in the aqueous environment, given the repulsion of these (Wyatt et al., 2011; Zhong et al., 2013). With the addition of salt, there is the screening effect of the added ions and the consequent balance of the charges of the biopolymer molecules, promoting the reduction of the repulsion between them, however the availability of polymers and the consequent proximity due to the high concentration of the gum enables the formation new connections between molecules in the environment (Wyatt et al., 2011; Zhong et al., 2013; Wyatt and Liberatore, 2010). In addition, the small divalent ions, as in the case of calcium cations, enter the intramolecular spaces of the polymer chains and act as a non-covalent lattice, favoring the formation of bonds between the particles dispersed in the environment, increasing the viscosity (Wyatt and Liberatore, 2010). In this scenario, the addition of salt increases the viscosity of the XG solution (Wyatt et al., 2011; Wyatt and Liberatore, 2010). In parallel, in view of a possible sedimentation of XG molecules with a high concentration of salts, despite the turbidity in XG solutions with concentrations greater than 0.1% (m/v) under the addition of NaCl (Morariu et al., 2018), there are records of sedimentation of the polymer by adding this salt (Morariu et al., 2018; García-Ocho et al., 2000). Xie and Lecourtier (1992) demonstrated stability of XG solutions in concentrations greater than 0.2% (m/v) for the addition of up to 2% (m/v) of $CaCl_2$, at 25°C. In addition, to preserve the flow according to the proposed rheological model, Wyatt and Liberatore (2009) determined that salt-free XG solutions, with concentrations between 20 and 70ppm, presented shear thinning, and concentrations above 70ppm presented minimal stress with proportional growth increased XG concentration. In addition, Melo (2008) determined that, for concentrations greater than 0.34% (m/v), salt-free XG solutions have thixotropy.

The selected NA concentrations come from the historic usage of nanoparticles for the development of nanofluids: for fluids based on clay, usually under a clay concentration of 7% (m/v), 0.1% to 2% (m/v) nanoparticle (Vryzas and Kelessidis, 2017; Kelessidis et. al, 2009; Bera and Belhaj, 2016). For XG solutions, William et al. (2014) and Ponmani et al. (2014) used between 0.1 to 0.5% m/v for solutions of 0.4% (m/v) of XG; Perween et al. (2019) adopted nanoparticles concentrations between 0.05% to 0.3% (m/v) in GX solutions of 0.25% (m/v). In this study, the NA concentrations varied between 0.005% to 1% (m/v). The concentrations of NA in the evaluated samples are shown in Table 2. It is observed that the first sample does not present the addition of NA, exactly to serve as a reference for the increase of rheological parameters.

Table 3 shows the shear stress values obtained in the tests for each sample. It is observed that, for a wide range of NA concentrations, only the concentration range between 0.05%, 0.1%, 0.125% and 0.15% (m/v) shows an increase in shear stresses, when compared to the sample free of nanoparticle. For example, the shear stress for $19.44s^{-1}$ of the NA-free sample (sample I) is 7.560Pa and increases to 10.017Pa in sample III (0.05% w/v), an increase of 32.5%. Samples IV, XI and XII show an increase for this same shear rate of 22.5%, 47.50% and 50.0%, respectively. It is also observed that, for sample III, the stress increase is negative by 1.14% for $1574.4s^{-1}$, meaning that the NA-free sample, with a final stress of 24.854Pa, changes to 24.570Pa, however this difference corresponds at 284mPa, which can be considered irrelevant. The same occurs with the increase in sample IV, which adds the same 1.14% in stress to the respective shear rate. Therefore, it can be considered that such samples practically alter the initial stresses of XG, preserving the final stress of the fluid. Samples XI and XII, on the other hand, show a greater increase in shear stress in all shear rates, the most significant being 0.15% (m/v) of NA. It is also observed, in this scenario, that the main contribution to the flow was the increase of the initial stresses, which means a greater resistance to flow for fluid at rest, characteristic of Bingham plastics, a model widely foreseen for drilling fluids based on clay (Kelessidis et al., 2006; Kelessidis et al., 2007; Kelessidis and Maglione, 2008), but less present in XG-based fluids (Borges et al., 2009; Speers and Tung, 1986; Khalil and Jan, 2012). Figures 3A, 3B and 3C show, respectively, the shear rate curves by shear stress for samples whose concentrations vary from 0.0% to 0.025% (m/v), 0.05% to 0.125% (m/v) and 0.15% to 1.0%. Figure 3D shows the shear rate curves by shear stress for samples I, III, IV, XI and XII, to highlight the increment on the stresses recorded from the addition of NA.

Table 2 - NA concentration in the samples analyzed in the rheology test.

Samples	I	VIII	II	IX	III	X	IV	XI	XII	V	VI	VII
NA Concentration (% m/v)	0.00	0.005	0.010	0.025	0.050	0.075	0.100	0.125	0.150	0.250	0.500	1.000

Source: Authors.

Table 3 - Shear Stress obtained by adding NA.

Shear Rate (s^{-1})	Shear Stress (Pa)											
	I	VIII	II	IX	III	X	IV	XI	XII	V	VI	VII
19.440	7.560	8.930	7.371	7.938	10.017	7.749	9.261	11.151	11.340	9.450	8.694	8.930
32.400	8.222	9.781	8.127	10.301	10.679	8.411	9.923	11.718	12.191	10.017	9.545	9.781
58.320	9.450	10.560	9.356	9.828	11.624	9.545	10.773	12.380	13.325	10.962	10.206	10.560
97.200	10.679	11.553	10.679	11.151	12.663	10.773	12.002	13.797	14.459	12.002	11.813	11.553
174.96	12.380	13.254	12.285	12.947	13.986	12.380	13.797	15.309	16.301	13.797	13.514	13.254
291.60	14.553	14.742	14.364	14.837	15.876	13.892	15.593	17.105	18.144	15.498	15.498	14.742
524.90	17.388	17.010	17.010	17.388	18.333	16.160	18.333	19.940	20.837	18.144	17.955	17.010
874.80	20.412	19.420	19.751	20.318	20.790	18.333	21.074	22.397	23.672	20.696	20.696	19.420
1574.4	24.854	22.822	23.436	24.665	24.570	22.019	25.137	26.555	28.208	24.570	24.665	22.822

Source: Authors.

Figure 3 - Shear Stress Rate for samples with concentrations between 0.0% (Pure XG) and 0.025% (m/v) (A); for samples with a concentration between 0.05% and 0.125% (m/v) (B); for samples with a concentration between 0.150% and 1,000% (m/v) (C); Shear Stress Rate for samples III, IV, XI and XII.
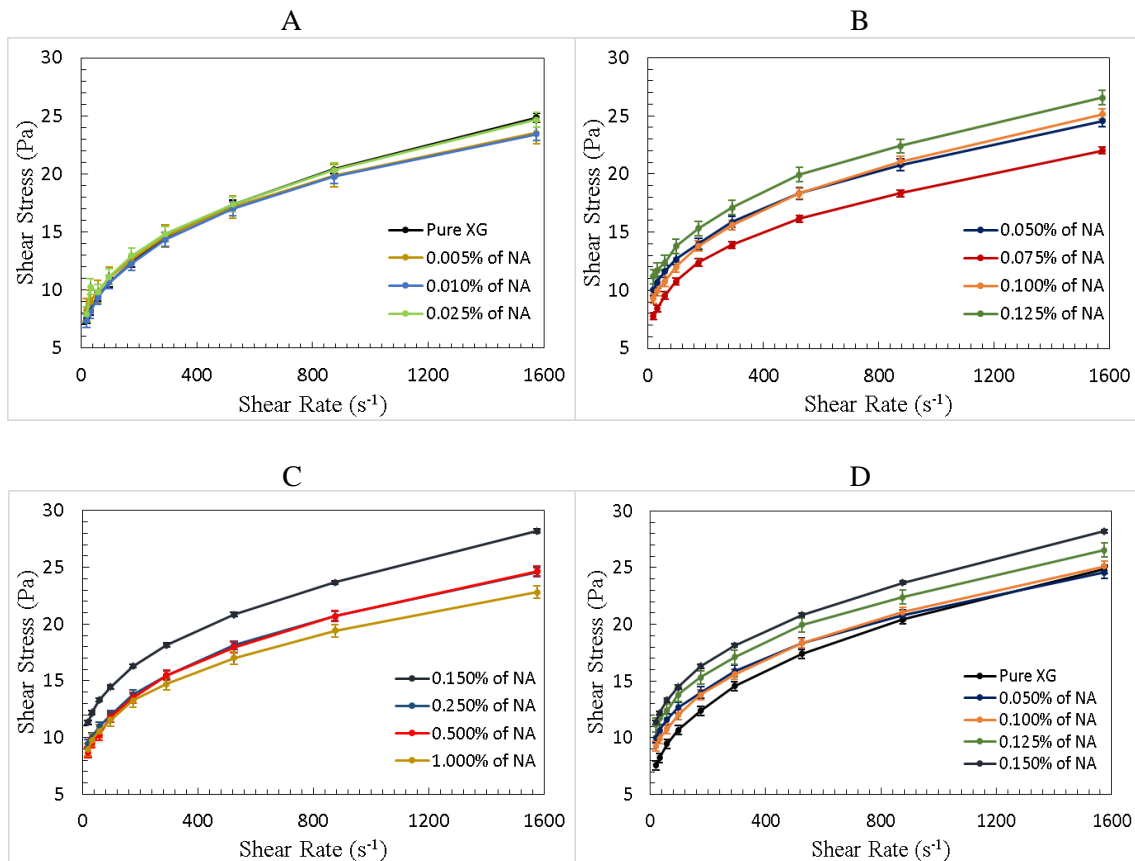

Source: Authors.

It is also observed that, with the increase in the shear rate, the increase in shear stresses decreases, following the shear thinning phenomenon, common for pseudoplastic fluids, expected for XG solutions (Holme et al., 1988; Khalil and Jan, 2012; Wyatt and Liberatore, 2009). Such decrease follows a logarithmic relationship for each measured concentration. Although the increase in stress is perceived for the respective concentration range, a law was not observed that links the concentration of NA with the increase in stress. Table 4 shows the percentage increase for each measured stress, relative to samples III, IV, XI and XII. Figure 4 shows the evolution of the percentage increase on shear stresses for samples III, IV, XI and XII: it is verified that, by the trend line, the logarithmic behavior of the phenomenon. Frame 1 shows the equations for the respective curves in Figure 4.

Table 4 - Percentage increase on the shear stress measured for each shear rate, in relation to the stresses verified in the NA-free sample.

Shear Rate (s^{-1})	Samples			
	III	IV	XI	XII
19.440	32.50%	22.50%	47.50%	50.00%
32.400	29.89%	20.69%	42.53%	48.28%
58.320	23.00%	14.00%	31.00%	41.00%
97.200	18.58%	12.39%	29.20%	35.40%
174.96	12.98%	11.45%	23.66%	31.68%
291.60	9.09%	7.14%	17.53%	24.68%
524.90	5.43%	5.43%	14.67%	19.84%
874.80	1.85%	3.24%	9.72%	15.97%
1574.4	-1.14%	1.14%	6.84%	13.50%

Source: Authors.

Figure 4 - Percentage increase on the Shear Stresses of the NA-free sample.
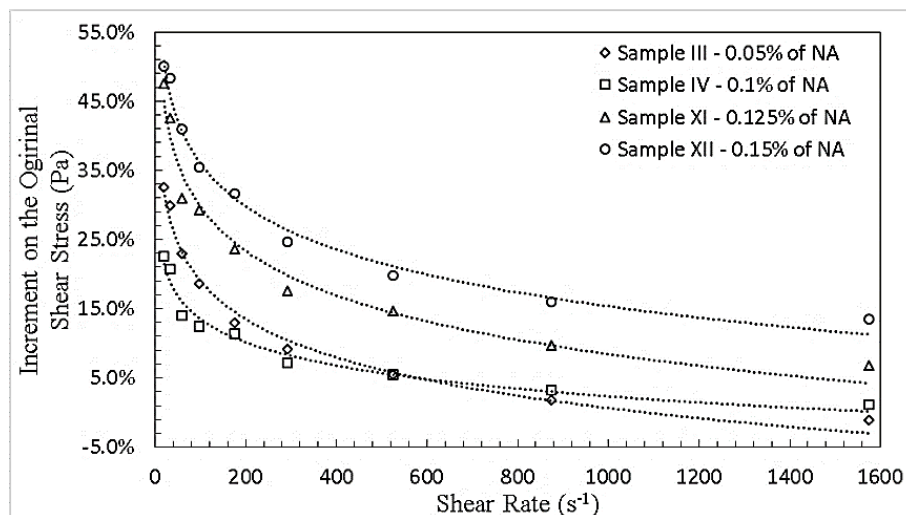
Source: Authors.

Frame 1 - Mathematical models for the percentage increments on the Shear Stresses of the NA-free sample.

Samples	Equations	R^2
III	$y = -0.08\ln(x) + 0.5581$	0.9896
IV	$y = -0.049\ln(x) + 0.359$	0.9705
XI	$y = -0.093\ln(x) + 0.7243$	0.9750
XII	$y = -0.09\ln(x) + 0.7736$	0.9889

Source: Authors.

Still with a view to increasing the shear stress of XG solutions, the rheological parameters of the samples in question were evaluated. Table 5 shows the values obtained for the rheological parameters of samples III, IV, XI and XII. Again, a law was not observed that would associate the values of the calculated parameters with the variation of the NA mass.

Table 5 - Values of the rheological parameters and correlation coefficient calculated under the Herschel-Bulkley rheological model, for samples III, IV, XI and XII.

Amostras	I	III	IV	XI	XII
k (Pa.s^n)	0.9428	0.7485	0.8628	0.7230	0.8914
n	0.4103	0.4169	0.4112	0.4289	0.4122
τ_0 (Pa)	4.0502	7.2159	5.9944	8.2013	8.1429
R^2	0.9999	0.9997	0.9997	0.9991	0.9998

Source: Authors.

It is observed that the Behavior Index remains practically constant with the addition of NA: the average of the values obtained was 0.4173, with an amplitude of 4.25% over the average, a standard deviation of 1.39%; when compared to the value of the parameter for an NA-free sample, the difference between the average value and the respective is 1.71%. Therefore, it can be concluded that the value of this parameter is preserved with the addition of the nanoparticle, that is, the addition does not interfere with the pseudoplastic behavior of the sample, meaning the prevalence of the rheological properties of XG before NA, as already verified by other authors (Xie and Lecourtier, 1992; Benyounes et al., 2010).

The Consistency Index changed with the addition of NA. It was found that the addition reduced the parameter by 20% for samples with 0.05% and 0.125% (m/v), and by less than 10% for samples with 0.1% and 0.15% (m/v). The viscosity of the polymer in a nanoparticle-free solution comes from its concentration in the environment as well as from the crosslinking effect caused by the cations dispersed in the solution (Wyatt et al., 2011; Zhong et al., 2013; Wyatt and Liberatore, 2010). This phenomenon can be justified by the presence of the silanol group on the surface of the nanoparticle (Rojtanatanya and Pongjanyakul, 2010; Rongthong et al., 2013) which, in addition to being the link with the hydroxyls of the biopolymer, forms links with the water in the environment (Maghzi et al., 2014), which facilitates the mobility between the particles during the stress of shearing, which is interesting for drilling fluids as it ensures less mechanical effort to raise the gravel to the surface (Caenn et al., 2014; Abu-Jdayil, 2011; Vryzas et al., 2016).

The Minimum Stress of the samples increased to 50% or more in relation to the value of the initial parameter, reaching double the value for samples XI and XII. This characteristic was required in XG solutions, precisely because of thixotropy, a property associated with gravel support when the drilling fluid is at rest (Caenn et al., 2014; Abu-Jdayil, 2011; Vryzas et al., 2016). XG solutions free of polyvalent cations and in low concentration, do not present a network formation because of the great electrostatic repulsion of the macromolecules; this repulsion is mitigated by the high concentration of cations in the environment and by the high concentration now worked out experimentally (Wyatt et al., 2011; Zhong et al., 2013; Wyatt and Liberatore, 2010), however, it cannot be admitted that, even if mitigated, this repulsion does not exist in these conditions. This perspective is ratified by the change in parameter values after the addition of the nanoparticle: due to the large surface area, which is essentially formed by silanol groups (Santos, 1989; Rojtanatanya and Pongjanyakul, 2010; Rongthong et al., 2013), a the presence of NA enhances the formation of hydrogen bonds between the particles of the biopolymer, and of these with the water, intensifying the formation of a network.

3.3. Part 3

In this step, the concentrations of XG, NaCl and $CaCl_2$ in the mixture were maintained. Also, in view of the concentrations that showed an increase over the rheological parameters, sample IV was adopted as a reference, whose NA concentration

was 0.10% (m/v). The temperatures worked were 25°C, 42°C, 59°C and 72°C. The temperature ceiling adopted was intended to prevent water loss through evaporation.

In the absence of salt, the XG in an aqueous environment, at a temperature below 51°C, dispersed by electrostatic repulsion and has a disordered fractured helix conformation; with increasing temperature, there is a conformational change from XG to a coil-like structure, which disrupts the XG structure (Rocheford and Middleman, 1987; Choppe et al., 2010; Luporini and Bretas, 2011). This conformational change reduces the viscosity and shear thinning of XG solutions, bringing their rheological behavior closer to Newtonian fluids (Speers and Tung, 1986; Borges et al., 2009). The addition of salt minimizes the electrostatic repulsion of the trisaccharide chains, making the molecules adopt a double-helix structure ordered in the form of rods; minimizing electrostatic repulsion allows the interaction between molecules by XG hydrogen bonds (Rocheford and Middleman, 1987; Choppe et al., 2010; Luporini and Bretas, 2011); this interaction allows the conformational transition temperature to be greater than 51°C (Luporini and Bretas, 2011). For example, Luporini and Bretas (2011) determined that there was no conformational transition for temperatures below 86°C. Xie and Lecourtier (1992) verified in suspensions of 1% XG (m/v) with bentonite, for concentrations of 2% NaCl (m/v) or 1% $CaCl_2$ (m/v), conformational transition temperature 125°C - it should also be considered that bentonite does not interfere with XG's conformational transition temperature (Xie and Lecourtier, 1992). Consequently, the rheological properties in XG saline solutions are less influenced by the increase in temperature (Xie and Lecourtier (1992); Rocheford and Middleman, 1987; Choppe et al., 2010).

Figure 5 shows the shear stress rate curves of the samples with 0.1% NA, for each measured temperature. Table 6 presents the results of stress by shear rate adopted for each temperature. Table 7 shows the proportion of the shear stress reduction for each temperature range and in relation to the initial temperature. It is observed that, at a temperature lower than the conformational change of salt-free XG solutions, there is a reduction in the shear stress for higher shear rates. For example, between temperatures 25°C and 42°C, there is no stress reduction to $19.44s^{-1}$, but there is a 2% reduction for the following shear rates; the reduction progresses to the shear rate of $1574.4s^{-1}$, on the order of 11.3%. When the phenomenon is observed between 42°C and 59°C, it can be seen that the reduction is more significant over the whole range, but marked in the initial and final shear rates - between 12.62% to 15.82% -, and for the other shear rates, varying between 8.83% and reaching 10.97%. For the transition between 59°C and 76°C, the phenomenon

remains, with more marked reductions for the higher shear rates - in the order of 7.54% to 10.56% -, an average reduction of 5.49% between $32.4s^{-1}$ and $291.6s^{-1}$, and a negligible reduction for first stress, less than 1%. It is also observed that, when compared to the shear stress at 25°C, the reduction is more pronounced: the reduction for the initial stresses, at $19.44s^{-1}$, are of the order of 15% for 59°C and 76°C; stress in the intermediate rates are already rising to 10.53%, reaching 16.36% to 59°C, and growing even more to 76°C, reaching almost 22%; for final rate stresses, the reduction varies between 18.04% to 59°C, reaching 28.57% to 76°C. These results can be justified by the high concentration of XG in the environment which, even under the presence of a large amount of salts, and considering the independence of NA over the rheological effects suffered by XG in the face of temperature variation, ends up suffering a partial degradation as an increase temperature, even if in a reduced form.

Figure 5 – Shear Rate by Shear Stress, for each measured temperature.
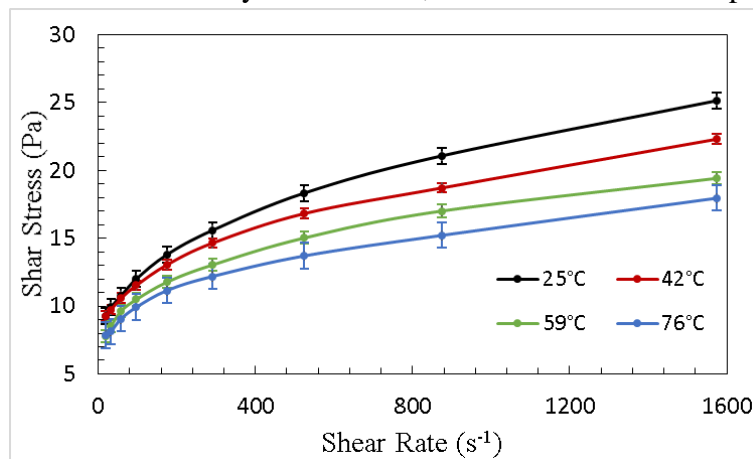
Source: Authors.

Table 6 - Effect of the temperature increase on the mixtures shear stresses with 0.1% (m/v) of NA.

Shear Rate (s^{-1})	Shear Stress (Pa)			
	25ºC	42ºC	59ºC	76ºC
19.440	9.261	9.261	7.796	7.844
32.400	9.923	9.734	8.505	8.127
58.320	10.773	10.584	9.639	9.072
97.200	12.002	11.529	10.490	9.923
174.96	13.797	13.041	11.765	11.151
291.60	15.593	14.648	13.041	12.191
524.90	18.333	16.821	15.026	13.703
874.80	21.074	18.711	17.010	15.215
1574.4	25.137	22.302	19.420	17.955

Source: Authors.

The previous analysis should be extended to the rheological parameters of the mixtures, shown in Table 8. In the transition between 25°C and 42°C, a 5.58% decrease in the Consistency Index is observed, a 5.61% increase over the Minimum Stress , and a 4.20% reduction in the Behavior Index. This phenomenon can be interpreted as a greater availability of biopolymer molecules dispersed in the environment, caused by the increase in temperature; this provides a greater interaction between the particles when at rest, but less resistance to flow when in motion, causing even greater shear thinning. This phenomenon is similar to what happened with lamellar structures, such as those of bentonite, which, with the increase in temperature, suffers from these structures due to the release of adsorbed water, causing sedimentation (Santos, 1989; Xie and Lecourtier, 1992); this sedimentation causes greater mechanical resistance to flow at rest, but less resistance to shear (Xie and Lecourtier, 1992). In the transition between 42°C and 59°C, there is an increase of 104.83% in the Consistency Index, a reduction of 43.84% in the Minimum Stress and a reduction of 24.13% in the Behavior Index. This phenomenon, already seen by Rocheford and Middleman (1987), can be justified under the same perspective of XG conformational change: with conformational change, the disorderly structure, in great concentration, should provide a greater mechanical impediment to shear flow and consequent less shear thinning, but it should reduce the interaction of the structures when at rest. For the transition between 59°C and 76°C, there is a 42.88%

reduction in the Consistency Index, an increase of 39.13% in the Minimum Stress and an increase of 15.44% in the Behavior Index. This can be justified in analogy to bentonite suspensions (Santos, 1989; Xie and Lecourtier, 1992): with the increase in temperature, there are more disordered molecules and a greater energy of water molecules on the surface of the nanoparticles given the temperature of the environment, which decreases the ability to resist shear and consequently offer less thinning by thinning; at rest, there is greater availability of dispersed particles, but interactions are weak, especially due to Van der Walls (Luporini and Bretas, 2011), since hydrogen bridges are no less viable by agitating water molecules and the disordered structure of molecules of XG.

Another relevant analysis occurs on the variations of the parameters in relation to those determined at 25°C: in the transition to 42°C, the variation of the parameters was in the order of 4% to 5%. Comparing the parameters determined at 25°C and 59°C, there is an increase of 93.41% in the Consistency Index, in addition to reductions of 27.31% in the Behavior Index and 40.69% in the Minimum Stress, showing the effect of the conformational change (Rocheford and Middleman, 1987; Choppe et al., 2010; Luporini and Bretas, 2011) and, consequently, weaker interactions between particles dispersed in the environment, greater mechanical impediment to flow and greater resistance to shear thinning. When comparing the parameters obtained at 25°C and 76°C, there is an increase of 10.47% for the Consistency Index, and reductions of 16.09% for the Behavior Index and 17.48% for the Minimum Stress, therefore, milder changes compared to the changes observed at 59°C. Certainly, due to the proximity to the temperature of conformational change, the disorganized particles must be closer and, consequently, they must offer greater mechanical impediment to shear than at higher temperatures, where there is certainly less interaction with water, more spacing between macromolecules and greater mobility between scattered particles. For this reason, the increase over the parameters is greater when close to the transition temperature and milder when moving away.

Table 7 - Proportion of shear stress reduction with increasing temperature: evaluation for each temperature range.

Shear Rate (s⁻¹)	Δτ (%) – between temperature ranges				
	25°C→42°C	25°C→59°C	25°C→76°C	42°C→59°C	59°C→76°C
19.440	0.00%	-15.82%	-15.31%	-15.82%	+0.61%
32.400	-1.90%	-14.29%	-18.10%	-12.62%	-4.44%
58.320	-1.75%	-10.53%	-15.79%	-8.93%	-5.88%
97.200	-3.94%	-12.60%	-17.32%	-9.02%	-5.41%
174.96	-5.48%	-14.73%	-19.18%	-9.78%	-5.22%
291.60	-6.06%	-16.36%	-21.82%	-10.97%	-6.52%
524.90	-8.25%	-18.04%	-25.26%	-10.67%	-8.81%
874.80	-11.21%	-19.28%	-27.80%	-9.09%	-10.56%
1574.4	-11.28%	-22.74%	-28.57%	-12.92%	-7.54%

Source: Authors.

Table 8 - Values of the rheological parameters and correlation coefficient: effect of the temperature increase on the rheological parameters, for the mixture with 0.1% NA.

Rheological Parameters	Temperature			
	25°C	42°C	59°C	76°C
k (Pa.s^n)	0.8628	0.8147	1.6687	0.9531
n	0.4112	0.3940	0.2989	0.3450
τ_0 (Pa)	5.9944	6.3304	3.5553	4.9465
R^2	0.9997	0.9991	0.9996	0.9983

Source: Authors.

On the other hand, the effect of saline "shielding" with conformational change should not be considered to be null. It is observed that, even with a variation of apparent viscosity (Consistency Index) and flow Minimum Stress, especially the shear thinning (Behavior Index) are still relatively preserved: evaluating the variation of the shear stress with those of NA-free sample, it is observed that, for 42°C, the stresses remain higher until the last three shear rates; the variation is more significant at 59°C and 76°C, when they increase by up to 3.75% for the initial rates, but decrease by up to 27.76% for the finals. The same is noticed when rheological parameters are evaluated: the Behavior Index, at 42°C, decreases by 13.58% in relation to the parameter of the exempt sample, increases by 77% by 59°C and increases by 1.1% at 76°C; the Minimum Stress increases by 56.3% at 42°C, decreases by 12.22% at 59°C and increases by 22.13% at 76°C; the Behavior Index reduces by 4% at 42°C, by 27% at 59°C and by 16% at 76°C, but it does not grow, tending to Newtonian behavior. It is noticed that, even with the reduction of shear stress and variations of rheological parameters, the fluid still presents binghanian and pseudoplastic behavior. This behavior was verified by Howard et al. (2015) and Reinoso et al. (2019) for XG concentrations in different saline solutions.

Comparing the results with similar studies, Melo (2008), for mixtures of XG at 84% (w/v) with additives that include NaCl, baryte and MgO_2, evaluating the influence of temperature on the rheological parameters, observed an increase of 32.5% in the Consistency Index between 25°C and 45°C, but losses of approximately 12.5% in the other parameters; considering the average of the results at 55 and 65°C and comparing them with those at 45°C, he observed losses of 32.5%, 8.5% and 19% for the Consistency Index, Behavior Index and Minimum Stress, respectively; there was no evaluation at a temperature above 65°C; comparing the results obtained from the transition between 55

and 65°C, there was a reduction of 66%, 9.8% and 16% for the respective parameters. Comparing the two studies, considering the proximity of the temperatures of 42 and 45°C and both being below the temperature of conformational change, a smaller reduction of the parameters is observed for the samples with NA; for an average range of 60°C, this relationship is reversed, with more significant reductions in the Behavior Index and Minimum Stress for samples with NA, but an increase of 104% over the Consistency Index for the nanofluid compared to a reduction of 27% for the sample of Melo (2008). In addition, the reductions in the rheological parameters between 55°C and 65°C are more pronounced for the study by Melo (2008) than those observed in the transition of the nanofluid parameters both between 42 and 59°C, and between 59 and 76°C. Therefore, it can be concluded that the increase in temperature causes a disorganization of the XG particles, but the presence of nanoclay in the mixture allows the recovery of the interactions of these particles, and consequently, the recovery of the rheological properties of the fluid. Therefore, samples with NA are less sensitive to temperature variation over their rheological parameters.

3.4. Part 4

In this step, the same concentrations of the components of the mixture as in the previous step were adopted. The influence of the hydration time of the samples on the shear stresses and on the rheological parameters of the Herschel-Bulkley model was evaluated. To this end, it is emphasized that Melo (2008) separately verified the effect on XG solutions and bentonite suspensions, attesting that XG solutions stabilize their rheological parameters within 24 hours of hydration, but the bentonites did not do so in 120h of evaluation. Santos (1989) points out that the effect on bentonite comes from the great hygroscopic capacity of the clays, which incorporate abundant water to their structure, given the presence of the silanol group (Santos, 1989). This effect occurs mainly in the clays of the montmorillonite group, the same clay from the nanoparticle adopted in this study. Table 9 shows the variation in shear stresses under the hydration time of the samples.

It is observed that the shear stress variations were small, under a standard deviation that ranged from 1,767% to 4,246%, meaning the predominance of XG rheology over NA (Xie and Lecourtier, 1992; Benyounes et al., 2010) and a certain stability in the rheological behavior of the mixture over the measured period. This can be

justified by the nanoparticulate state of the clay, which does not cause the effect of water incorporation over time (Santos, 1989; Melo, 2008): the nanoparticle, for being under a lamellar structure (Santos, 1989; Golubeva et al., 2013; Uddin, 2008; Hoidy et al. 2009) and by the interaction with the other components of the mixture, its particles end up being kept apart from each other, which prevents the incorporation of water between the valleys formed between the lamellae. The nanoparticle interaction occurs mainly with the biopolymer trisaccharides by hydrogen bonding with the NA silanol group, and by this type of bonding with the solution's free water (Santos, 1989; Rojtanatanya and Pongjanyakul, 2010; Rongthong et al., 2013; Maghzi et al., 2014).

The same behavior is observed for the evaluated rheological parameters, shown in Table 10. It is noticed that the Behavior Index varies between 0.3758 and 0.4112, under an average of 0.3949 and a standard deviation of 3.6%, a certain stability for the interval of measured time. The Minimum Stress fluctuated between 5.9944 and 7.4238Pa, an average of 6.6430Pa and a standard deviation of 7.84%, which can be explained by the dynamic interaction between the particles that form hydrogen bonds and their Brownian motion in the environment. The Consistency Index varied more significantly, between 834.5 and 1188.9mPa.s^n, an average of 991.7mPa.s^n and standard deviation of 14.9%, but which can also be justified in analogy to the Minimum Stress.

Table 9 - Influence of sample hydration time on shear stress.

Shear Rate (s^{-1})	Shear Stress (Pa)								
	24h	48h	72h	96h	120h	144h	Average	S. Deviation	S. Deviation (%)
19.440	9.261	9.923	10.206	10.301	9.734	9.923	9.891	0.263	2.654%
32.400	9.923	10.631	11.246	11.435	10.962	10.348	10.757	0.457	4.246%
58.320	10.773	11.907	12.191	12.474	11.813	11.340	11.750	0.462	3.932%
97.200	12.002	13.041	13.514	13.986	13.230	12.899	13.112	0.465	3.544%
174.96	13.797	14.884	14.742	15.593	14.837	14.459	14.718	0.394	2.675%
291.60	15.593	16.727	16.538	17.294	16.821	16.443	16.569	0.378	2.281%
524.90	18.333	19.278	18.995	19.940	19.278	19.136	19.160	0.339	1.767%
874.80	21.074	22.255	21.452	22.680	22.019	21.546	21.837	0.480	2.200%
1574.4	25.137	26.366	25.704	27.027	26.271	25.657	26.027	0.528	2.027%

Source: Authors.

Table 10 - Influence of the hydration time on the rheological parameters of the mixture.

Rheological Parameters	Hydration time (h)					
	24	48	72	96	120	144
k (Pa.s^n)	0.8628	1.0725	0.8345	1.1889	1.1570	0.8345
n	0.4112	0.3884	0.4081	0.3758	0.3780	0.4081
τ_0 (Pa)	5.9944	6.2617	7.4238	6.6280	6.1265	7.4238
R^2	0.9997	0.9999	0.9989	0.9992	0.9994	0.9989

Source: Authors.

3.5. Part 5

In order to verify the interaction between the saline ions dispersed in the solution with the NA and XG particles, the influence of the NA concentration in the XG saline solutions and the hydration time on the Electrical Conductivity and the Zeta Potential were evaluated. For the first evaluation, two samples were selected that presented discrepant rheological parameters, comparing them with the 0.1% NA sample (m/v). For the second evaluation, samples of 0.1% NA (w/v) between 24 and 144h of hydration were evaluated. The results of the two evaluations are shown in Tables 11 and 12, respectively.

Considering that Electrical Conductivity is a measure of free ion distribution in the environment subject to electrical conduction, it can be inferred that they would be in dynamic balance of interaction between ions and counterions dispersed in the aqueous environment (Rao et al., 2005), which makes it an indirect measure of interaction between the particles in the mixture. In parallel, it should be considered that, in polyelectrolyte saline solutions, the electrical conductivity of the environment is practically independent of the polyelectrolyte concentration for high salt concentrations (Sagou et al., 2015; Bordi and Carnetti, 1986). From the results presented in the two evaluations, it is observed that the concentration of electrolytes in equilibrium is practically stable: the conductivity values for the samples showed a maximum difference of 6%, which means that this balance does not depend on the variation of NA in the environment; for variation of hydration time, the results vary by 5% between 24 and 120h, with only a discrepancy in these values in the 144h sample; the values for this hydration time can be considered null, since they vary between zero and -1.0mS/cm.

Table 11 - Influence of increased NA concentration on Electrical Conductivity and Zeta Potential.

Samples	Concentration (m/V)	Zeta Potential (mV)			Conductivity (mS/cm)			k (Pa.s^n)	n	τ_0 (Pa)
IV	0.100%	9.86	98.9	37.9	172	172	172	0.8628	0.4112	5.9944
IX	0.025%	0.914	6.41	-4.94	182	182	182	0.6582	0.4442	5.8685
II	0.010%	-16.7	-34.6	-6.86	172	172	173	1.5059	0.3475	2.7919

Source: Authors.

Table 12 - Influence on the hydration time on the Electrical Conductivity and the Zeta Potential of the sample with 0.1% NA (m/v).

Time (h)	Zeta Potential (mV)			Conductivity (mS/cm)			k (Pa.s^n)	n	τ_0 (Pa)
144	-1.49	-3.14	-4.01	-0.117	-0.246	-0.315	0.8345	0.4081	7.4238
120	-4.38	2.53	-7.89	174.0	175.0	175.0	1.1570	0.3780	6.1265
96	-6.68	8.53	-28.3	178.0	180.0	180.0	1.1889	0.3758	6.6280
72	-0.582	-17.7	42.5	174.0	175.0	175.0	0.8345	0.4081	7.4238
48	42.7	-0.275	29.9	180.0	181.0	181.0	1.0725	0.3884	6.2617
24	9.86	98.9	37.9	172.0	172.0	172.0	0.8628	0.4112	5.9944

Source: Authors.

It is important to mention that Electrical Conductivity attests only to the concentration of electrolytes with sufficient electrophoretic mobility to conduct electric current, therefore it does not discriminate the charge or the type of electrolyte (Roa et al., 2005; Show, 1992); the stability measured in the experiment points to a stability in the ionic concentration in the environment, but not to the dynamics of the interactions. For this, the Zeta Potential was measured, which corresponds to the electrophoretic mobility of the particles dispersed in the environment and also adopted as a measure of stability between the particles; this property is sensitive to the concentration and charge of the electrolytes in the environment (Shaw, 1992). For XG solutions, the Zeta Potential varies between -20 and -74mV, in proportion to the increase in the concentration of the biopolymer, since it is anionic (Thonart et al., 1985). In parallel, it should be noted that the instability interval between flocculation and deflocculation occurs between ± 50mV (Salopek et al., 1992).

Evaluating the results of the samples with different concentrations of NA, it is observed that the sample IV presents electrophoretic stability, even with great variations of Zeta Potential. However, the same was not verified for samples II and IX, whose transitions of the parameter values between positive and negative suggest instability in the interactions of the particles of the environment (Shaw, 1992; Salopek et al. 1992). It is also verified that the increase in the concentration of NA negatively interferes in the interaction between the cations and the biopolymer molecules, which is reflected in the values of Zeta Potential varying from negative to positive with the increase in NA concentration, pointing to a greater availability of cations with mobility in the mixture. The previous results demonstrate the total interaction between nanoparticles and biopolymer. This perspective can be associated with the rheological parameters of the samples in question: for 24h of hydration, the sample with 0.01% (m/v) of NA presents, even in the interval of instability, negative values of the parameter, demonstrating an anionic predominance of the solution; the sample with 0.025% (m/v) shows values that change between positive and negative, and the sample with 0.1% (m/v) shows positive values. This fact justifies the transition observed in the rheological parameters of the samples in question: for the sample with 0.01% NA, with little availability of nanoparticles, there is a predominance of fragile interactions naturally promoted between the polymer molecules (Wyatt et at., 2011; Zhong et al., 2013; Wyatt and Liberatore, 2010), reflected in the high value of the Consistency Index and the low value of the Minimum Stress; in the sample with 0.025% NA, with greater availability of

nanoparticles in the environment, the formation of hydrogen bonds and reduction of the interaction between the polymer molecules during the stress application   given the connection with water is favored (Rojtanatanya and Pongjanyakul, 2010; Rongthong et al., 2013; Maghzi et al., 2014), which explains the decrease in the Consistency Index and the increase in Minimum Stress; in the sample to 0.1% (m/v), for intermediate values to those presented between the previous and the following sample.

The increase in the hydration time reduces the values of Zeta Potential: initially varying between 9.89 and 98.9mV, the values tend to change between positive and negative in 48h of hydration already, a fact that intensifies at the end of the period, whose amplitude reduces ± 10mV in the penultimate of close to zero in the last period. This result can be interpreted as a lower availability of ions with mobility in the environment over time, justified by the possible interaction of cations with nanoparticles (Santos, 1989) and/or with XG molecules still with free anionic regions (Wyatt et at., 2011; Zhong et al., 2013; Wyatt and Liberatore, 2010), to the point of almost exhausting them from the environment. It is observed that the value of Electrical Conductivity is also close to zero, which would correspond to almost total interaction of the dispersed ions, in the absence of conductivity or ion mobility. This justification is confirmed by the stability of the rheological parameters of the samples for the measured hydration interval, allowing to conclude that the available cations do not interfere in the binding of NA with XG molecules.

4. Final Considerations

It was concluded that, for an analyzed concentration range, the nanoclay increases the shear stresses of saline solutions of XG in the concentrations 0.05%, 0.10%, 0.125% and 0.15% (m / v). There was a certain reduction in dynamic viscosity (Consistency Index) of a maximum of 20%, but there was a substantial increase in viscosity at rest (Minimum Tension), increases that even doubled this parameter. It was also observed that the main increases in shear stress occur in the initial shear rates, tending to decrease with increasing rate. These results allow us to conclude that the nanoparticles positively interfere in the ability to form bonds between the XG macromolecules when at rest, increasing their binghanian characteristic, even improving the thixotropy of the solution. The addition of the nanoparticle does not interfere with the pseudoplastic profile of the mixture, characteristic of XG solutions.

The temperature continues to act negatively on the properties of the solution, as it reduces the shear stresses, Behavior Index and Minimum Stress. These parameters even reduce 30% at 76ºC, showing that, even in the presence of salt, certainly due to the high concentration of XG, part of the particles undergo conformational change. The temperature also interferes with the Behavior Index, which fluctuates with its increase, however is not far from the pseudoplastic behavior. Comparing the parameters with previous studies, it is observed that the nanoparticle contributes positively to the preservation of the rheological parameters of the mixture.

It was also observed stability of the rheological parameters for the hydration time between 24h and 144h, meaning that the clay's dependence on hydration was already resolved. Therefore, it is concluded that the addition of NA favored the evaluated parameters, as well as their preservation with increasing temperature and their stability over the hydration time.

Finally, it was observed that there is an interaction between the particles of NA and XG, reflected in the change in the values of Zeta Potential with the increase of the concentration of the nanoclay and in the change of the rheological parameters. The sample with 0.1% (w/v) of nanoclay shows electrophoretic stability in 24h of hydration, however the reduction of the parameter to values close to zero, indicating that the solvated cations end up interacting with the biopolymer and /or the nanoclay to the point of almost runs out of them in the middle. This fact, however, does not affect the rheology of the mixture.

For future studies, it is interesting to evaluate the rheology of nanoclay and xanthan mixtures in saline solutions with trivalent ions, especially due to the sensitivity of xanthan the presence of high ionization ions (Kelco, 2000). Another suggestion is the evaluation of the rheology of the mixture worked in this research under high pressure at high temperature. Another, the evaluation of the filtrate of the mixture adopted in this work.

References

Abdou, M. I. & Ahmed, H. E.-S. (2011). Effect of particle size of bentonite on rheological behavior of the drilling mud. *Petrol. Sci. Technol., 29*(21), 2220–2233. doi: 10.1080/10916461003663065

Abu-Jdayil, B. (2011). Rheology of sodium and calcium bentonite–water dispersions: Effect of electrolytes and aging time. *Int. J. Miner. Process., 98*(3-4), 208–213. doi: 10.1016/j.minpro.2011.01.001

Aftab, A, Ismail, A. R., Ibupoto, Z. H., Akeiber, H. & Malghani, M. G. K. (2017). Nanoparticles based drilling muds a solution to drill elevated temperature wells: A review. *Renew. Sust. Energ. Rev., 76*, 1301–1313. doi: 10.1016/j.rser.2017.03.050

Alizadeh, S., Sabbaghi, S. & Soleymani, M. (2015). Synthesis of Alumina/Polyacrylamide nanocomposite and its influence on viscosity of drilling fluid. *Int. J. Nano Dimens., 6*(3), 271-276. doi: 10.7508/IJND.2015.03.006

Al-Yasiri, M., Awad, A., Pervaiz, S. & Wen, D. (2019). Influence of silica nanoparticles on the functionality of water-based drilling fluids. *J. Petrol. Sci. Eng., 179*, 504–512. doi: 10.1016/j.petrol.2019.04.081

Al-Yasiri, M. S. & Al-Sallami, W. T. (2015). How the Drilling Fluids Can be Made More Efficient by Using Nanomaterials. *Am. J. Nano Res. Appl., 3*, 41-45. doi: 10.11648/j.nano.20150303.12

Amanullah, M., Al-Arfaj, M. K. & Al-Abdullatif, Z. A. (2011, March 1-3). Preliminary test results of nano-based drilling fluids for oil and gas field application. Paper presented at the *SPE/IADC Drilling Conference and Exhibition*. Amsterdam: Society of Petroleum Engineers.

Amiri, M. C. & Sadeghialiabadi, H. (2014). Evaluating the Stability of Colloidal Gas Aphrons in the Presence of Montmorillonite Nanoparticles. *Colloid. Surface. A, 457*, 212-219. doi: 10.1016/j.colsurfa.2014.05.076

Amorim, L.V. (2003). *Melhoria, Proteção e Recuperação da Reologia de Fluidos Hidroargilosos para Uso na Perfuração de Poços de Petróleo*. (Doctoral Thesis). Universidade Federal de Campina Grande, Campina Grande, PB.

Barry, M. M., Jung, Y., Lee, J. -K., Phuoc, T. X. & Chyu, M. K. (2015). Fluid filtration and rheological properties of nanoparticle additive and intercalated clay hybrid bentonite drilling fluids. *J. Petrol. Sci. Eng., 127*, 338–346. doi: 10.1016/j.petrol.2015.01.012

Benyounes, K., Mellak, A. & Benchabane, A. (2010). The Effect of Carboxymethylcellulose and Xanthan on the Rheology of Bentonite Suspensions. *Energy Source. Part A, 32*(17), 1634–1643. doi: 10.1080/15567030902842244

Bera, A. & Belhaj, H. (2016). Application of nanotechnology by means of nanoparticles and nanodispersions in oil recovery - A comprehensive review. *J. Nat. Gas Sci. Eng., 34*, 1284-1309. doi: 10.1016/j.jngse.2016.08.023

Bordi, F. & Carnetti, C. (1986). Equivalent Conductivity of Carboxymethylcellulose Aqueous Solutions with Divalent Counterions. *J. Phys. Chem., 90*(13), 3034-3038. doi: 10.1021/j100404a049

Borges, C. D., Vendruscolo, C. T., Martins, A. L.; Lomba, R. F. T. (2009). Comportamento Reológico de Xantana Produzida por Xanthomonas arboricola pv pruni para Aplicação em Fluido de Perfuração de Poços de Petróleo. *Polimeros, 19*(2), 160-165. doi: 10.1590/S0104-14282009000200015

Caenn, R., Darley, H. C. H. & Gray, G. R. (2014). *Fluidos de Perfuração e Completação* (6 ed.). Rio de Janeiro, RJ: Elsevier B. V..

Cheraghian, G. (2017). Application of Nano-Particles of Clay to Improve Drilling Fluid. *Int. J. Nanosci. Nanotechnol., 13*(2), 177-186.

Cheraghian, G., Wu, Q., Mostofi, M., Li, M. -C., Afrand, M. & Sangwai, J.S. (2018). Effect of a Novel Clay/silica Nanocomposite on Water-Based Drilling Fluids: Improvements in Rheological and Filtration Properties. *Colloid. Surface. A, 555*, 339-350. doi: 10.1016/j.colsurfa.2018.06.072

Choppe, E., Puaud, F., Nicolai, T. & Benyahia, L. (2010). Rheology of xanthan solutions as a function of temperature, concentration and ionic strength. *Carbohydr. Polym., 82*(4), 1228–1235. doi: 10.1016/j.carbpol.2010.06.056

Chung, Y. -L. & Lai, H. -M. (2010). Preparation and properties of biodegradable starch-layered double hydroxide Nanocomposites. *Carbohydr. Polym., 80*(2), 525–532. doi: 10.1016/j.carbpol.2009.12.020

Comba, S., Dalmazzo, D., Santagata, E. & Sethi, R. (2011). Rheological characterization of xanthan suspensions of nanoscale iron for injection in porous media. *J. Hazard. Mater., 185*(2-3), 598–605. doi: 10.1016/j.jhazmat.2010.09.060

Contreras, O., Hareland, G., Husein, M., Nygaard, R. & Al-Saba, M. (2014, February 26-28). Application of in-house prepared nanoparticles as filtration control additive to reduce formation damage. Paper presented at the *SPE International Symposium and Exhibition on Formation Damage Control*. Lafayette, LA: Society of Petroleum Engineers. doi: 10.2118/168116-MS

Dolez, P. I. (2015). *Nanoengineering: Global Approaches to Health and Safety Issues* (pp. 3-40). Amsterdam: Elsevier B. V..

Energy Information Administration. (2017, September 14). *EIA projects 28% increase in world energy use by 2040*. Retrieved March 27, 2020, from https://www.eia.gov/todayinenergy/detail.php?id=32912.

Energy Information Administration. (2006, June). *International Energy Outlook 2006*. Retrieved March 28, 2020, from http://www.economicswebinstitute.org /essays/energy2006.pdf

Fakoya, M. F. & Shah, S. N. (2013, March 26-27). Rheological Properties of Surfactant-Based and Polymeric Nano-Fluids. Paper presented at the *SPE/ICoTA Coiled Tubing and Well Intervention Conference and Exhibition*. The Woodlands, TX: Society of Petroleum Engineers. doi: 10.2118/163921-MS

Fitzgerald, B. L., McCourt, A. J. & Brangetto, M. (2000, February 23-25). Drilling Fluid Plays Key Role in Developing the Extreme HTHP, Elgin/Franklin Field. Paper presented at the *IADC/SPE Drilling Conference*. New Orleans, LA: Society of Petroleum Engineers. doi: 10.2118/59188-MS

Gaidzinski, R., Osterreicher-Cunha, P., Duailibi Fh., J. & Tavares, L. M. (2009) Modification of clay properties by aging: Role of indigenous microbiota and implications for ceramic processing. *Appl. Clay Sci., 43*(1), 98–102. doi: 10.1016/j.clay.2008.07.007

García-Ochoa, F., Santos, V. E., Casas, J. A. & Gómez, E. (2000). Xanthan gum: production, recovery, and properties. *Biotechnol. Adv., 18*(7), 549-579. doi: 10.1016/S0734-9750(00)00050-1

Gierszewska, M., Jakubowska, E. & Olewnik-Kruszkowska, E. (2019). Effect of chemical crosslinking on properties of chitosan-montmorillonite composites. *Polym. Test., 77*, 105872. doi: 10.1016/j.polymertesting.2019.04.019

Golubeva, O. Y., Ul'yanova, N. Y., Kostyreva, T. G., Drozdova, I. A. & Mokeev, M. V. (2013). Synthetic Nanoclays with the Structure of Montmorillonite: Preparation, Structure, and Physico-Chemical Properties. *Glass Phys. Chem+, 39*(5), 533–539. doi: 10.1134/S1087659613050088

Grim, R. E. & Güven, N. (1978). *Bentonites: Geology, Mineralogy, Properties and Uses Developments in Sedimentology* (24 ed.). Amsterdam: Elsevier Scientific Publishing Company.

Hassani, A. H & Ghazanfari, M. H. (2017). Improvement of non-aqueous colloidal gas aphron-based drilling fluids properties: Role of hydrophobic nanoparticles. *J. Nat. Gas Sci. Eng., 42*, 1-12. doi: 10.1016/j.jngse.2017.03.005

Herschel, W. H. & Bulkley, R. (1926). Konsistenzmessungen von Gummi-Benzollösungen. *Kolloid-Z.*, 39, 291–300.

Hoelscher, K. P., Stefano, G. D., Riley, M. & Young, S. (2012, June 12-14). Application of nanotechnology in drilling fluids. Paper presented at the *SPE International Oilfield Nanotechnology Conference and Exhibition*. Noordwijk: Society of Petroleum Engineers. doi: 10.2118/157031-MS

Hoidy, W. H., Ahmad, M. B., Al Mulla, E. A. J. & Ibrahim, N. A. B. (2009). Synthesis and Characterization of Organoclay from Sodium Montmorillonite and Fatty Hydroxamic. *Acids. Am. J. Appl. Sci., 6*(8), 1567-1572. doi: 10.3844/ajassp.2009.1567.1572

Holme, K. R., Hall, L. D, Speers, R. A. & Tung, M. A. (1988). High shear rate flow behavior of xanthan gum dispersions. *Food Hydrocoll., 2*(2), 159-167. doi: 10.1016/S0268-005X(88)80014-6

Howard, S., Kaminski, L. & Downs, J. (2015, June 3-5). Xanthan stability in formate brines - Formulating non-damaging fluids for high temperature applications. Paper presented at the *SPE European Formation Damage Conference and Exhibition*. Budapest: Society of Petroleum Engineers. doi: 10.2118/174228-MS

Ismail, A. R., Aftab, A., Ibupoto, Z. H. & Zolkifile, N. (2016). The novel approach for the enhancement of rheological properties of water-based drilling fluids by using multi-walled carbono nanotube, nanosilica and glass beads. *J. Petrol. Sci. Eng., 139*, 264–275. doi: 10.1016/j.petrol.2016.01.036

Jain, R. & Mahto, V. (2015). Evaluation of polyacrylamide/clay composite as a potential drilling fluid additive in inhibitive water based drilling fluid system. *J. Petrol. Sci. Eng., 133*, 612–621. doi: 10.1016/j.petrol.2015.07.009

Jang, H. Y., Zhang, K., Chon, B. H. & Choi, H. J. (2015). Enhanced oil recovery performance and viscosity characteristics of polysaccharide xanthan gum solution. *J. Ind. Eng. Chem., 21*, 741–745. doi: 10.1016/j.jiec.2014.04.005

Kelco, C. Q. (2000). *Xanthan gum book* (8 ed.). Atlanta, GA: C. Q. Kelco.

Kelessidis, V. C. & Maglione, R. (2008). Yield stress of water–bentonite dispersions. *Colloid. Surface. A, 318*(1-3), 217–226. doi: 10.1016/j.colsurfa.2007.12.050

Kelessidis, V. C., Maglione, R., Tsamantaki, C. & Aspirtakis, Y. (2006). Optimal determination of rheological parameters for Herschel–Bulkley drilling fluids and impact on pressure drop, velocity profiles and penetration rates during drilling. *J. Petrol. Sci. Eng., 53*(3-4), 203–224. doi: 10.1016/j.petrol.2006.06.004

Kelessidis, V. C., Papanicolaou, C. & Foscolos, A. (2009). Application of Greek lignite as an additive for controlling rheological and filtration properties of water–bentonite suspensions at high temperatures: A review. *Int. J. Coal Geol., 77*(3-4), 394–400. doi: 10.1016/j.coal.2008.07.010

Kelessidis, V. C., Tsamantaki, C. & Dalamarinis, P. (2007). Effect of pH and electrolyte on the rheology of aqueous Wyoming bentonite dispersions. *Appl. Clay Sci., 38*(1-2), 86–96. doi: 10.1016/j.clay.2007.01.011

Kennedy, J. R. M., Kent, K. E. & Brown, J. R. (2015). Rheology of dispersions of xanthan gum, locust bean gum and mixed biopolymer gel with silicon dioxide nanoparticles. *Mat. Sci. Eng. C, 48*, 347–353. doi: 10.1016/j.msec.2014.12.040

Khalil, M. & Jan, B. M. (2012). Herschel-Bulkley Rheological Parameters of a Novel Environmentally Friendly Lightweight Biopolymer Drilling Fluid from Xanthan Gum and Starch. J. *Appl. Polym. Sci., 124*(1), 595–606. doi: 10.1002/app.35004

Khodja, M., Canselier, J. P., Bergaya, F., Fourar, K., Khodja, M., Cohaut, N. & Bemounah, A. (2010). Shale problems and water-based drilling fluid optimisation in the Hassi Messaoud Algerian oil field. *Appl. Clay Sci., 49*(4), 383-393. doi: 10.1016/j.clay.2010.06.008

Khunawattanakul, W., Puttipipatkhachorn, S., Rades, T. & Pongjanyakul, T. (2010). Chitosan–magnesium aluminum silicate nanocomposite films: Physicochemical characterization and drug permeability. *Int. J. Pharm., 393*(1-2), 219–229. doi: 10.1016/j.ijpharm.2010.04.007

Laird, D. A. (2006). Influence of layer charge on swelling of smectites. *Appl. Clay Sci., 34*(1-4), 74–87. doi: 10.1016/j.clay.2006.01.009

Li, M., Wu, Q., Song, K., Hoop, C. F. D., Lee, S., Qing, Y. & Wu, Y. (2016). Cellulose Nanocrystals and Polyanionic Cellulose as Additives in Bentonite Water-Based Drilling Fluids: Rheological Modeling and Filtration Mechanisms. *Ind. Eng. Chem. Res., 55*(1), 133–143. doi: 10.1021/acs.iecr.5b03510

Liu, H., Nakagawa, K., Chaudhary, D., Asakuma, Y. & Tadé; M. O. (2011). Freeze-dried macroporous foam prepared from chitosan/xanthan gum/montmorillonite nanocomposites. *Chem. Eng. Res. Des., 89*(11), 2356–2364. doi: 10.1016/j.cherd.2011.02.023

Lucena, D. V., Lira, H. L. & Amorim, L. V. (2014). Efeito de aditivos poliméricos nas propriedades reológicas e de filtração de fluidos de perfuração. *Tecnol. Metal Mater. Miner., 11*(1), 66-73. doi: 10.4322/tmm.2014.010

Luporini, S. & Bretas, R. E. S. (2011). Caracterização Reológica da Goma Xantana: Influência de Íons Metálicos Univalente e Trivalente e Temperatura em Experimentos Dinâmicos. *Polimeros, 21*(3), 188-194. doi: 10.1590/S0104-14282011005000043

Maghzi, A., Kharrat, R., Mohebbi, A. & Ghazanfari, M. H. (2014). The impact of silica nanoparticles on the performance of polymer solution in presence of salts in polymer flooding for heavy oil recovery. *Fuel, 123*, 123–132. doi: 10.1016/j.fuel.2014.01.017

Mariani, F. Q., Villalba, J. C. & Anaissi, F. J. (2013). Caracterização Estrutural de Argilas Utilizando DRX com Luz Síncrotron, MEV, FTIR e TG-DTG-DTA. *Orbital: Electronic J. Chem., 5*(4), 249-256.

Melo, C., Garcia, P. S., Grossmann, M. V. E., Yamashita, F., Dall'Antônia, L. H. & Mali, S. (2011). Properties of Extruded Xanthan-Starch-Clay Nanocomposite Films. *Braz. Arch. Biol. Technol., 54*(6), 1223-1333. doi: 10.1590/S1516-89132011000600019

Melo, K. C. (2008). *Avalição e modelagem reológica de fluidos de perfuração base água* (Master's Thesis). Universidade Federal do Rio Grande do Norte, Natal, RN.

Mélo, T. J. A., Araújo, E. M., Brito, G. F. & Agrawal, P. (2014). Development of nanocomposites from polymer blends: effect of organoclay on the morphology and mechanical properties. *J. Alloy Compd., 615*, S391-S391. doi: 10.1016/j.jallcom.2013.11.151

Menezes, R. R., Melo, L. R. L., Fonseca, F. A. S., Ferreira, H. S., Martins, A. B. & Neves, G. A. (2008). Caracterização de argilas bentoníticas do Município de Sussego, Paraíba, Brasil. *Revista Eletrônica de Materiais e Processos, 3*(2), 36-43.

Monteiro, S. N. & Vieira, C. M. F. (2004). Influence of firing temperature on the ceramic properties of clays from Campos dos Goytacazes, Brazil. *Appl. Clay Sci., 27*(3-4), 229–234. doi: 10.1016/j.clay.2004.03.002

Morariu, S., Bercea, M. & Brunchi, C.-E. (2018). Phase separation in xanthan solutions. *Cellul. Chem. Technol., 52*(7-8), 569-576.

Morita, R. Y., Barbosa, R. V. & Kloss, J. R. (2015). Caracterização de Bentonitas Sódicas: Efeito do Tratamento com Surfactante Orgânico Livre de Sal de Amônio. *Rev. Virtual Quim.,7*(4),1286-1298. doi: 10.5935/1984-6835.20150071

Nejad, M. H., Ganster, J., Bohn, A., Volkert, B. & Lehmann, A. (2011). Nanocomposites of starch mixed esters and MMT: Improved strength, stiffness, and toughness for starch propionate acetate laurate. *Carbohydr. Polym., 84*(1), 90–95. doi: 10.1016/j.carbpol.2010.10.067

Noori, S., Kokabi, M. & Hassan, Z. M. (2015). Nanoclay Enhanced the Mechanical Properties of Poly(Vinyl Alcohol)/Chitosan/Montmorillonite Nanocomposite Hydrogel as Wound Dressing. *Procedia Mater. Sci., 11*, 152–156. doi: 10.1016/j.mspro.2015.11.023

Oueslati, W., Ammar, M. & Chorfi, N. (2015). Quantitative XRD Analysis of the Structural Changes of Ba-Exchanged Montmorillonite: Effect of an in Situ Hydrous Perturbation. *Minerals, 5*, 507-526. doi: 10.3390/min5030507

Parizad, A., Shahbazi, K. & Tanha, A. A. (2018). Enhancement of polymeric water-based drilling fluid properties using nanoparticles. *J. Petrol. Sci. Eng., 170*, 813–828. doi: 10.1016/j.petrol.2018.06.081

Perween, S., Thakur, N. K., Beg, M., Sharma, S. & Ranjan, A. (2019). Enhancing the properties of Water based Drilling Fluid using Bismuth Ferrite Nanoparticles. *Colloid. Surface. A, 561*, 165-177. doi: 10.1016/j.colsurfa.2018.10.060

Ponmani, S., William, J. K. M., Samuel, R., Nagarajan, R. & Sangwai, J. S. (2014). Formation and characterization of thermal and electrical properties of CuO and ZnO nanofluids in xanthan gum. *Colloid. Surface. A, 443*, 37–43. doi: 10.1016/j.colsurfa.2013.10.048

Pooja, D., Panyaram, S., Kulhari, H., Rachamalla, S. S. & Sistla, R. (2014). Xanthan gum stabilized gold nanoparticles: Characterization, Biocompatibility, Stability and Cytotoxicity. *Carbohydr. Polym., 110*, 1-9. doi: 10.1016/j.carbpol.2014.03.041

Prodanov, C. C. & Freitas, E. C. (2013). *Metodologia do Trabalho Científico: Métodos e Técnicas de Pesquisa e do Trabalho Acadêmico* (2nd ed., pp. 129-141). Feevale. http://www.feevale.br/Comum/midias/8807f05a-14d0-4d5b-b1ad-1538f3aef538/E-book%20Metodologia%20do%20Trabalho%20Cientifico.pdf

Rao, M. A., Rizvi, S. S. H. & Datta, A. K. (2005). *Engineering Properties of Foods* (3 ed, pp. 461-500). Boca Raton, FL: Taylor and Francis Group.

Reinoso, D., Martín-Alfonso, M. J., Luckham, P. F. & Martínez-Boza, F. J. (2019). Rheological characterisation of xanthan gum in brine solutions at high temperature. *Carbohydr. Polym., 203*, 103–109. doi: 10.1016/j.carbpol.2018.09.034

Riley, M., Young, S., Stamatakis, E., Guo, Q., Ji, L., Stefano, G. D., … & Friedheim, J. (2012, March 28-30). Wellbore stability in unconventional shales-the design of a

nanoparticle fluid. Paper presented at the *SPE Oil and Gas India Conference and Exhibition*. Mumbai, MH: Society of Petroleum Engineers. doi: 10.2118/153729-MS

Rochefort, W. E. & Middleman, S. (1987). Rheology of Xanthan Gum: Salt, Temperature, and Strain Effects in Oscillatory and Steady Shear Experiments. *J. Rheol., 31*, 337-369. doi: 10.1122/1.549953

Rojtanatanya, S. & Pongjanyakul, T. (2010). Propranolol-magnesium aluminum silicate complex dispersions and particles: characterization and factors influencing drug release. *Int. J; Pharm., 383*(1-2), 106-115. doi: 10.1016/j.ijpharm.2009.09.016

Rongthong, T., Sungthongjeen, S., Siepmann, J. & Pongjanyakul, T. (2013). Quaternary polymethacrylate-magnesium aluminum silicate films: molecular interactions, mechanical properties and tackiness. *Int. J; Pharm., 458*(1), 57-64. doi: 10.1016/j.ijpharm.2013.10.016

Sadeghalvaad, M & Sabbaghi, S. (2015). The Effect of the TiO2/Polyacrylamide Nanocomposite on Water-Based Drilling Fluid Properties. Powder Technol., 272, 113–119. doi: 10.1016/j.powtec.2014.11.032

Sagou, J. -P. S.; Ahualli, S. & Thomas, F. (2015). Influence of ionic strength and polyelectrolyte concentration on the electrical conductivity of suspensions of soft colloidal polysaccharides. *J. Colloid Interf. Sci., 459*, 212–217. doi: 10.1016/j.jcis.2015.08.001

Salopek, B., Krasić, D. & Filipović, S. (1992). Measurement and application of zeta-potential. *Rud.-geol.-naft. zb., 4*, 147-151.

Santos, P. S. (2000). *Tecnologia das Argilas: Fundamentos* (Vol. 1). São Paulo, SP: Edgard Blücher.

Santos, R. F. A., Reis, M. M., Ueki, M. M., Santos, Z. I. G. & Brito, G. F. (2016, November 6-10). Influência da argila montmorilonita nas propriedades mecânicas e morfológicas de nanocompósitos obtidos a partir de blendas de polietileno/poli

(tereftalato de etileno). Paper presented at the *22º Congresso Brasileiro de Engenharia e Ciência dos Materiais*. Natal, RN: Associação Brasileira de Cerâmica.

Sato, T., Watanabe, T. & Otsuka, R. (1992). Effects of layer charge, charge location, and energy change on expansion proprerties of dioctahedral smectites. *Clay. Clay Miner., 40*(1), 103-113. doi: 10.1346/CCMN.1992.0400111

Shakib, J. T., Kanani, V. & Pourafshary, P. (2016). Nano-clays as additives for controlling filtration properties of water - bentonite suspensions. *J. Petrol. Sci. Eng., 138*, 257-264. doi: 10.1016/j.petrol.2015.11.018

Shaw, D. J. (1992). *Colloid and Surface Chemistry* (4 ed., pp.174-243). Oxford: Elsevier Science Ltd.

Slavutsky, A. M., Bertuzzi, M. A. & Armada, M. (2012). Water barrier properties of starch-clay nanocomposite films. *Braz. J. Food. Technol., 15*(3), 208-218. doi: 10.1590/S1981-67232012005000014

Soliman, A. A., El-hoshoudy, A. N. & Attia, A. M. (2020). Assessment of xanthan gum and xanthan-g-silica derivatives as chemical flooding agents and rock wettability modifiers. *Oil Gas Sci. Technol., 75*(12). doi: 10.2516/ogst/2020004

Speers, R. A. & Tung, M. A. (1986). Concentration and Temperature Dependence of Flow Behavior of Xanthan Gum Dispersions. *J. Food Sci., 51*(1), 96-98. doi: 10.1111/j.1365-2621.1986.tb10844.x

Srivatsa, J. T. & Ziaja, M. B. (2011, November 15-17). An experimental investigation on use of nanoparticles as fluid loss additives in a surfactant-polymer based drilling fluids. Paper presented at the *International Petroleum Technology Conference*. Bangkok: Society of Petroleum Engineers. doi: 10.2523/IPTC-14952-MS

Taheri, A. & Jafari, S. M. (2019). *Biopolymer Nanostructures for Food Encapsulation Purposes* (Vol. 1, 1 ed., pp. 521-578). Amsterdam: Elsevier B.V.

Tang, X., Alavi, S. & Herald, T. J. (2008). Effects of plasticizers on the structure and properties of starch–clay. *Carbohydr. Polym., 74*(3), 552–558. doi: 10.1016/j.carbpol.2008.04.022

Thonart, Ph., Paquot, M., Hermans, L. & Alaoui, H. (1985). Xanthan production by Xanthomonas campestris NRRL B-1459 and interfacial approach by zeta potential measurement. *Enzyme Microb. Technol.,* 7(5), 235-238. doi: 10.1016/S0141-0229(85)80009-0

Uddin, F. (2008). Clays, Nanoclays, and Montmorillonite Minerals. *Metall. Mater. Trans. A Phys. Metall. Mater. Sci., 39*(A), 2804-2814.

Villaça, J. C., Silva, L. C. R. P., Barbosa, L. H. F., Rodrigues, C. R., Lira, L. M., Carmo, F. A., ... & Cabral, L. M. (2014). Preparation and characterization of polymer/layered silicate pharmaceutical nanobiomaterials using high clay load exfoliation processes. *J. Ind. Eng. Chem., 20*(6), 4094-4101.

Vipulanandan, C. & Mohammed, A. (2015). Effect of nanoclay on the electrical resistivity and rheological properties of smart and sensing bentonite drilling muds. *J. Petrol. Sci. Eng.*, *130*, 86-95. doi: 10.1016/j.petrol.2015.03.020

Vryzas, Z. & Kelessidis, V.C. (2017). Nano-Based Drilling Fluids: A Review. *Energies*, *10*(4), 540, 1-34. doi: 10.3390/en10040540

Vryzas, Z., Wubulikasimu, Y., Gerogiorgis, D. I. & Kelessidis, V. C. (2016). Understanding the Temperature Effect on the Rheology of Water-Bentonite Suspensions. *Annual Transactions - The Nordic Rheology Society, 24*, 199-208.

Wang, Y., Xiong, Y., Wang, J. & Zhang, X. (2017). Ultrasonic-assisted fabrication of montmorillonite-lignin hybrid hydrogel: highly efficient swelling behaviors and super-sorbent for dye removal from wastewater. *Colloid. Surface. A, 520*, 903-913. doi: 10.1016/j.colsurfa.2017.02.050

William, J. K. M., Ponmani, S., Samuel, R., Nagarajan, R. & Sangwai, J. S. (2014). Effect of CuO and ZnO nanofluids in xanthan gum on thermal, electrical and high pressure rheology of water-based drilling fluids. *J. Petrol. Sci. Eng., 117*, 15–27. doi: 10.1016/j.petrol.2014.03.005

Wyatt, N. B. & Liberatore, M. W. (2010). The effect of counterion size and valency on the increase in viscosity in polyelectrolyte solution. *Soft Matter, 6*(14), 3346–3352. doi: 10.1039/C000423E

Wyatt, N. B. & Liberatore, M. W. (2009). Rheology and Viscosity Scaling of the Polyelectrolyte Xanthan Gum. *J. Appl. Polym. Sci., 114*, 4076–4084. doi: 10.1002/app.31093

Wyatt, N. B., Gunther, C. M. & Liberatore, M. W. (2011). Increasing viscosity in entangled polyelectrolyte solutions by the addition of salt. *Polymer, 52*(11), 2437-2444. doi: 10.1016/j.polymer.2011.03.053

Xie, W. & Lecourtier, J. (1992). Xanthan behavior in water-fluid drilling fluids. *Polym. Degrad. Stabil., 38*(2), 155-164.

Xie, W., Gao, Z., Pan, W. P., Hunter, D., Singh, A. & Vaia, R. (2001). Thermal Degradation Chemistry of Alkyl Quaternary Ammonium Montmorillonite. *Chem. Mater., 13*(9), 2979-2990. doi: 10.1021/cm010305s

Yang, K. K., Wang, X. L. & Wang, Y. Z. (2007). Progress in Nanocomposite of Biodegradable Polymer. *J. Ind. Eng. Chem., 13*(4), 485-500.

You, Z., Mills-Beale, J., Foley, J. M., Roy, S., Odegard, G. M., Dai, Q. & Goh, S. W. (2011). Nanoclay-modified asphalt materials: Preparation and characterization. *Constr. Build. Mater., 25*(2), 1072–1078. doi: 10.1016/j.conbuildmat.2010.06.070

Zhong, L., Oostrom, M., Truex, M. J., Vermeul, V. R. & Szecsody, J. E. (2013). Rheological behavior of xanthan gum solution related to shear thinning fluid delivery for

subsurface remediation. *J. Hazard. Mater., 244–245*, 160–170. doi: 10.1016/j.jhazmat.2012.11.028

Percentage of contribution of each author in the manuscript

Felipe Menezes de Souza – 20%

Juliana Mikaelly Dias Soares – 20%

Helinando Pequeno de Oliveira – 20%

Isabel Cristina Rigoli – 20%

Samuel Luporini – 20%